Talanta 280 (2024) 126747

Contents lists available at ScienceDirect

Talanta

journal homepage: www.elsevier.com/locate/talanta

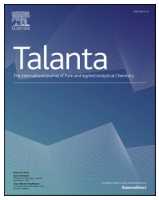

Exploring the analytical potential of total reflection X-ray fluorescence (TXRF) combined with partial least square (PLS) for simple determination of ash content in various coal types

Yongsheng Zhang [a,b], Jian Yuan [c], Rui Gao [a,b], Yang Zhao [d], Zefu Ye [e], Zhujun Zhu [e], Peihua Zhang [a,b], Lei Zhang [a,b,*], Wangbao Yin [a,b,**], Suotang Jia [a,b]

[a] State Key Laboratory of Quantum Optics and Quantum Optics Devices, Institute of Laser Spectroscopy, Shanxi University, Taiyuan, 030006, China
[b] Collaborative Innovation Center of Extreme Optics, Shanxi University, Taiyuan, 030006, China
[c] Beijing Research Institute of Uranium Geology, Beijing, 100029, China
[d] School of Semiconductor and Physics, North University of China, Taiyuan, 030051, China
[e] Shanxi Gemeng US-China Clean Energy R&D Center Co., Ltd., Taiyuan, 030032, China

A B S T R A C T

Ash content, as a crucial indicator of coal quality, its rapid and accurate determination is pivotal to improve the energy utilization of coal and reduce environmental pollution. Traditional spectroscopic methods face significant challenges in acquiring accurate information from coal samples due to the notorious matrix effects arising from their complex composition, vast molecular structure, and diverse coal types. In this study, the feasibility of total reflection X-ray fluorescence (TXRF) combined with partial least squares (PLS) for the determination of coal ash was firstly investigated based on the TXRF being unaffected by matrix effects. Firstly, coal samples were prepared as suspensions, and the effects of sample particle size and different dispersants on the results of TXRF analyses were evaluated. The accuracy and applicability of the chosen sample preparation strategies were further validated using inductively coupled plasma mass spectrometry (ICP-MS) and two certified reference materials (CRMs). Subsequently, based on the analysis of 19 coal samples, the impact of three different predictive variables on the performance of the PLS model was investigated: (a) TXRF full spectrum normalized by the net intensity of the internal standard; (b) net intensity of characteristic peaks for 12 elements (Al, Si, K, Ca, Ti, Fe, Cr, Mn, Cu, Ni, and Sr) normalized by the net intensity of the internal standard; (c) concentrations of the aforementioned 12 elements. The results demonstrate that the PLS model constructed usingthe TXRF full spectrum normalized by the net intensity of the internal standard exhibits the best predictive capabilities, with the determination coefficient of calibration set (R^2) and mean square error (MSE) of the prediction set reaching 0.9736 and 0.99 %, respectively. Moreover, the measurement accuracy of this model was six times greater than that obtained with traditional X-ray fluorescence (XRF). Presented analytical results display the possibilities of combining TXRF with PLS for coal quality evaluation.

1. Introduction

Coal is a complex solid fuel composed of combustible organic materials (primarily C, H, O, N, etc.) and non-combustible inorganic minerals (mainly Al, Si, Ca, Fe, etc.). It is widely utilized in various industrial fields, such as power generation and coking, etc. [1,2] To ensure a stable supply of energy and reduce the emission of environmental pollutants, strict control of coal quality is of particular importance.

Ash content serves as a key indicator of coal quality, indicating the level of inorganic minerals within the coal. Coals with high ash content contain substantial amounts of inorganic minerals, which are noncombustible and persist as residual ash after combustion. This not only diminishes the combustion performance but also lowers the thermal conductivity of the furnace. Therefore, it is essential to accurately determine the ash content of coal. Generally, the determination of ash content relies on the high-temperature ashing method, a rigorous technique that entails the complete oxidation of coal samples in a muffle furnace under controlled conditions. The ash content is subsequently quantified by measuring the mass difference before and after the combustion process. Despite its accuracy, this method is encumbered by

* Corresponding author. State Key Laboratory of Quantum Optics and Quantum Optics Devices, Institute of Laser Spectroscopy, Shanxi University, Taiyuan, 030006, China.
** Corresponding author. State Key Laboratory of Quantum Optics and Quantum Optics Devices, Institute of Laser Spectroscopy, Shanxi University, Taiyuan, 030006, China.
E-mail address: k1226@sxu.edu.cn (L. Zhang).

https://doi.org/10.1016/j.talanta.2024.126747
Received 20 May 2024; Received in revised form 22 July 2024; Accepted 21 August 2024
Available online 22 August 2024

laborious sample pretreatment, prolonged burning time, and a complex operational procedure [3], which no longer meets the modern industrial demand for rapid coal quality evaluation. To address this challenge, a variety of techniques for rapid determination of coal ash content have been developed. Prompt gamma neutron activation analysis (PGNAA) emerged as an early adopted technology [4,5], offering high sensitivity, accuracy, and the ability to simultaneously analyze multiple elements. However, its dependence on a neutron source poses radiological risks. In recent years, the combination of laser-induced breakdown spectroscopy (LIBS) with partial least squares (PLS) regression has demonstrated superior performance in coal ash determination [6,7]. Despite this, the high-energy laser pulses striking the coal surface generate dust, potentially contaminating optical components and causing irreversible ablation damage [8]. On the other hand, the combination of wavelength dispersive X-ray fluorescence (WDXRF) with interpretive machine learning algorithms provides a clear understanding of the contribution of inorganic components in coal samples to ash content, significantly propels ash content prediction research forward [9]. However, this technique, either WDXRF or energy dispersive X-ray fluorescence (EDXRF), is susceptible to the matrix effects of the sample [10]. To overcome the influence of matrix effects, a common approach is to calibrate the analysis using certified reference materials (CRMs) with a matrix composition similar to the samples being analyzed [11,12]. Alternatively, machine learning algorithms can be employed to reveal the correlations between spectral data and the target value in a large training dataset. Some popular machine learning algorithms, like random forest, can discern the impact of the sample matrix on the spectral signal and appropriately adjust for anomalies caused by the matrix effects.

Yet, these algorithms are typically considered as black-box models. This constraint makes it difficult to fully understand the operational mechanisms behind model corrections for matrix effects since these models do not transparently reveal the details of converting input data into output results. Consequently, there is a risk of overfitting, posing significant challenges to practical applications.

Total reflection X-ray fluorescence (TXRF) is a variant of EDXRF. Its advancement lies in the incidence of X-ray onto the sample film at an angle smaller than the critical angle (≈0.1°) [13], resulting in the phenomenon of total reflection. Consequently, the penetration depth is reduced to just a few nanometers [14], which considerably reduces the contribution of Compton and Rayleigh scattering to the spectral background. The detection limits (DLs) are improved by three orders of magnitude compared to EDXRF [15]. Importantly, as the photons carrying elemental characteristic information almost entirely originate from the sample surface, the so-called matrix effects are significantly weakened or even completely eliminated [13,16,17], greatly simplifying the process of elemental quantitative analysis. TXRF quantitative analysis typically employs the internal standard (IS) method, where a known concentration of an element is added to the target sample to correct for factors affecting measurement accuracy and precision, such as particle size, sample thickness, and grazing angle [18]. Owing to these advantages, we hypothesize that the relationship between elemental content and fluorescence intensity in coal samples can be accurately obtained using TXRF, avoiding the necessity of matrix effects correction. Thus, even with a limited dataset, it is possible to establish a connection between the complete composition and ash content of coal samples using machine learning algorithms, which will be an attractive study.

In this paper, the feasibility of using TXRF combined with PLS for the determination of ash content in various types of coal within a limited dataset was investigated. To our knowledge, this is the first attempt to combine TXRF with PLS for coal ash content measurement, and the results effectively evaluate the potential application of this method across a diverse range of coal samples. For this purpose, all coal samples were prepared as suspensions to determine the optimal sample preparation strategy, and the best predictive variables for PLS modeling were assessed. Furthermore, a comparative analysis with XRF was conducted to validate the suitability and accuracy of the proposed approach.

2. Experiment

2.1. Reagents

For TXRF analysis, the following materials were used: a mono-elemental standard solution of Ga (C = 1000 μg mL^{-1}, Guobiao (Beijing) Testing & Certification, China) for the preparation of IS; nono-ionic detergent 1 % Triton X-100 (Analytical Reagent, BIOISCO, China) and ethylene glycol (chromatographic purity Reagents, Macklin, China) were used as dispersants for the suspension procedure; deionized water (18.2 MΩ, Beijing research institute of uranium geology labwater), deconex weak alkaline cleaner (Borer chemie Ag, Switzerland), 68 % nitric acid (Aladdin, China) were used for cleaning the sample carrier; and silicone solution in isopropanol (SERVA, Germany) was applied for hydrophobization of the sample carrier.

2.2. Coal sample

To evaluate the analytical performance of the combined TXRF with PLS for the determination of coal ash, 19 coal samples from Shanxi Sunlight Coking (Shanxi, China) were used. Specific details about the samples, including the results of ash content analysis, are presented in Table 1. These samples cover 8 different coal ranks, including anthracite, bituminous, fertilization coal, etc. All coal samples have a particle size of less than 168 μm. In particular, Al, Si, Ca, Fe, Mn, and Ni in YG_1 were determined using inductively coupled plasma mass spectrometry (ICP-MS) following complete digestion with perchloric acid, hydrofluoric acid, and other acid reagents in the laboratory. Additionally, two CRMs, ZBM1101 (coal gangue) and ZBM1212 (coal ash), were employed in this study. These materials were exclusively used for validation of our analytical method, and will not be included as predictor variables in the construction of the ash prediction model.

2.3. Analysis with the TXRF

In TXRF analysis, two principal pretreatment strategies are typically applied for solid samples: suspension preparation and acid digestion. Suspension preparation method, involving thoroughly mixing solid powder with dispersants and IS solution, offers a simple and time-efficient process for TXRF analysis. However, the results may be subject to particle size effect [19]. In contrast, acid digestion completely dissolves the sample powder into solution using various acid reagents. This ensures a more uniform distribution of the IS within the sample, and eliminates the particle size effect [20]. However, owing to the complex matrix of coal samples, the acid digestion process is intricate and time-consuming [21,22]. Considering the need for rapid analysis, this study adopted the suspension preparation method as the pretreatment method for coal samples.

The process of preparing coal sample suspension is displayed in Fig. 1. It mainly consists of placing 10 mg of the sample with particle size I (<25 μm) or II (<168 μm) in a 2 mL centrifuge tube. Then, 1 mL of dispersant and 100 μL of a 1000 μg mL^{-1} Ga as IS were added. The

Table 1
Number, type and ash value of coal samples in the experiment.

Coal Number	Coal type	Range of ash values (%)
YG_1-5	anthracite	10.54–31.80
YG_6-7	bituminous	6.35–11.74
YG_8-11	fertilization coal	10.13–13.35
YG_12-13	lean coal	8.94–11.20
YG_14-16	gas coal	7.45–8.06
YG_17	coking coal	10.26
YG_18	gangue	23.50
YG_19	coal slime	65.53

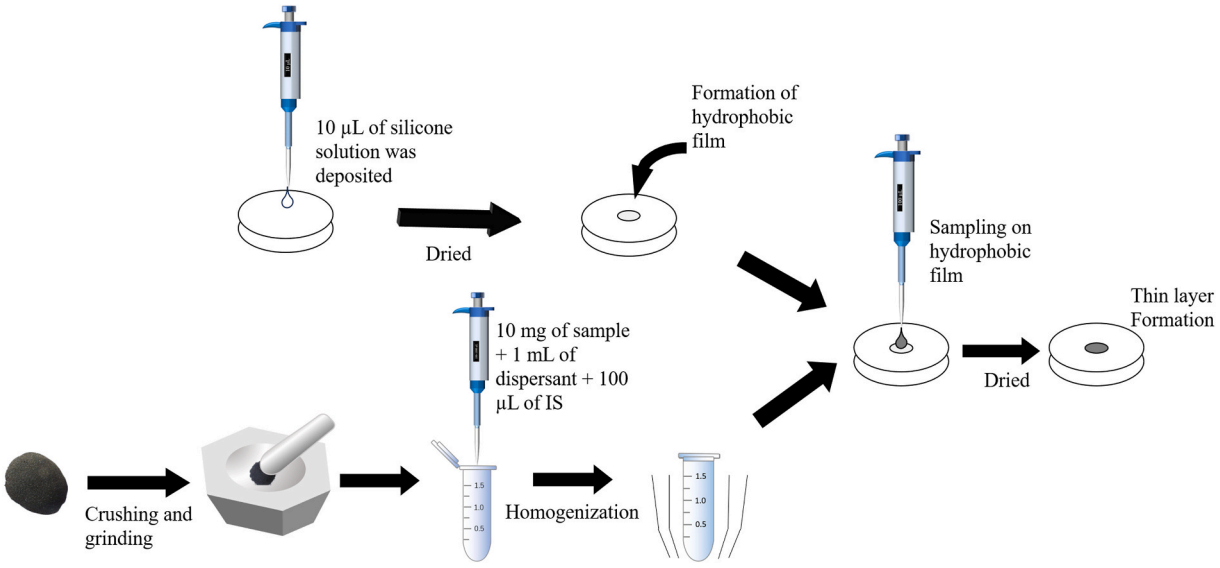

Fig. 1. Preparation of coal sample thin-film using suspension method.

centrifuge tubes were sonicated for 3 min to reduce particle aggregation. Subsequently, the centrifuge tubes were homogenized at 850 rpm for 2 min using a vortex mixer to ensure an even distribution of the samples and IS in the suspension. Finally, 10 μL of the mixture was deposited onto a quartz reflector and dried at 70–80 °C.

All measurements were performed using a benchtop spectrometer S2 PICOFOX (Bruker, Germany). This instrument is equipped with a 50 W X-ray tube featuring a Mo anode, a 17.5 keV Ni/C multilayer monchromator, and a silicon drift detector (SDD) with a 30 mm^2 active area and an energy resolution of less than 150 eV at the Mn Kα line. Quartz disks (Bruker, Germany) of 30 mm diameter and 3 mm of thickness were employed as sample carriers. Operating conditions under air with a voltage of 50 kV and a current of 0.6 mA for 600 s per sample. Spectra 7 software was used for spectral analyses, which is capable of obtaining the intensity of the characteristic peaks of the target element and quantifying their content according to the next formula:

$$C_i = \frac{C_{IS} \cdot N_i \cdot S_{IS}}{N_{IS} \cdot S_i} \quad (1)$$

where C_{IS} is the concentration of IS; N_i and N_{IS} are the net intensity of target element and IS, respectively. S_{IS} and S_i are the relative sensitivity of target element and IS, respectively.

2.4. Anlaysis with the XRF

In this experiment, the coal samples with particle sizes below 25 μm were analyzed using the XRF instrument described in Ref. [23]. The setup was equipped with a 50 W Rh anode X-ray tube (VF-50J, VARIAN), an SDD (VIAMP, KETEK), a digital pulse processor, a hydrogen generator, a measurement chamber, and a sample cell (L × W × H, 100 mm × 10 mm × 3 mm). The hydrogen generator was responsible for providing a hydrogen environment for the measurement chamber. The collimated X-ray tube and SDD were installed at a 45° angle relative to the vertical direction on the opposite side of the measurement chamber. The Be window of the SDD was positioned 2 mm away from the sample. Measurements on samples were conducted at an operation voltage of 16 kV and 600 μA current, and per sample was measured for 1 min. To ensure the reliability of the analysis, the coal samples were spread evenly in the sample cell, scraped flat, and tested.

2.5. PLS regression

PLS, as a prominent branch of machine learning algorithms, its capability in predicting target values had amply demonstrated across numerous fields [23–25]. The core principle of PLS is to map both predictor and response variables into a latent variable space, maximizing the covariance between them. This process not only reduces the complexity of the data but also retains the greatest explanatory power for the response variables [26]. In this study, PLS models were constructed for TXRF and XRF. For the TXRF, three sets of predictor variables were used: the full spectrum information of coal samples normalized with an IS, the intensities of Al, Si, K, Ca, Ti, Fe, Cr, Mn, Cu, Zn, Ni, and Sr normalized using an IS, and the contents of the previously mentioned 12 major and trace elements. Meanwhile, the XRF model was established using the total spectrum of coal samples. In both models, the coal ash content served as the response variable. The models were constructed in a Python environment, and hyperparameters within the PLS models, such as the number of latent variables, were finely tuned through GridSearchCV to ensure the optimization of model performance.

2.6. Validation and statistical details

To evaluate the performance of the TXRF and the PLS model, all calculations were performed using the average results obtained by the standard method and the average concentrations from three replicate TXRF tests.

Predicted value of coal ash content	y_i
Actual value of coal ash content	$\hat{y}_i$
Average actual ash content of coal	$\bar{y}_i$
TXRF measured value	C_i
Reference value (ICP-MS or certified value)	$C_{ref.i}$
Calibration set coefficient	$R^2 = 1 - \frac{\sum_{i=1}^{j}(y_i - \hat{y}_i)^2}{\sum_{i=1}^{j}(y_i - \bar{y}_i)^2}$
Mean square error (MSE)	$MSE = \frac{\sum_{i}^{k}(y_i - \hat{y}_i)^2}{k}$
Recovery	$R_i(\%) = \left(\frac{C_{TXRF.i}}{C_{ref.i}}\right) \times 100\%$
Relative standard deviation (RSD)	$RSD(\%) = \left(\frac{\sqrt{\frac{\sum_{i=1}^{N}(C_i - \overline{C_i})^2}{N-1}}}{\overline{C_i}}\right) \times 100\%$

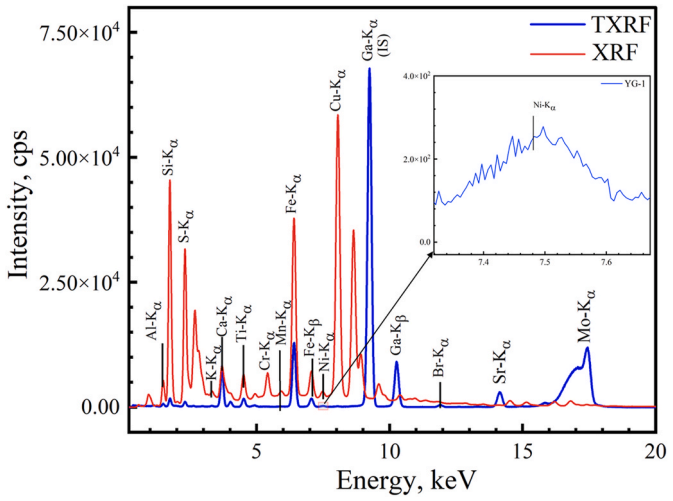

Fig. 2. TXRF and XRF generally spectrum of the YG_1.

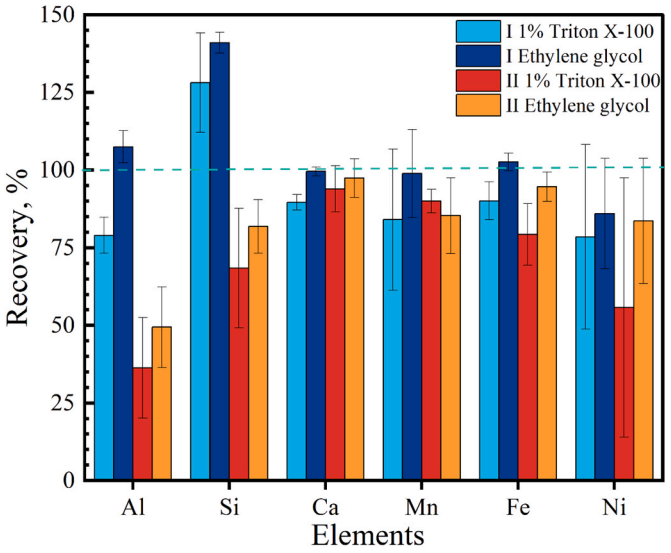

Fig. 3. The effect of sample particle size and dispersant type on the content of Al, Si, Ca, Mn, Fe and Ni in YG_1 (error bars represent the relative standard deviation of three parallel analyses of the sample).

3. Result and discussion

3.1. Investigation optimal coal sample analysis method

In TXRF analysis, particle size significantly impacts the stability of the suspension. Larger particles tend to sediment quickly in the suspension, leading to sedimentation heterogeneity and compromising sampling representativeness. Additionally, larger particles might obscure the effective excitation of small particles by X-rays during analysis. This spatial heterogeneity caused by the particle size effect can disrupt the uniformity of the X-ray fluorescence signal within the sample, thereby affecting the repeatability and accuracy of the analytical results. Therefore, investigating the optimal analytical particle size for coal sample preparation is crucial.

In this study, we used the YG_1 sample to investigate the influence of particle sizes I and II on the TXRF analytical results. Furthermore, the effectiveness of 1 % Triton X-100 and ethylene glycol as dispersants for the two different particle size samples were also evaluated. Samples were prepared as thin films according to the procedure described in section 2.3, and then analyzed by TXRF. Fig. 2 illustrates the TXRF spectrum of a YG_1. The results clearly demonstrated that Ga, serving as IS, exhibited a good response without interfering with the analysis of other elements, and no peak overlapping occurred among the elements. The sample primarily consisted of major elements such as Al, Si, Ca, and Fe, as well as trace elements like Mn, Ni, and Sr, all of which are closely associated with ash content. To investigate the suitable sample preparation strategy for coal sample analysis, we selected four major elements (Al, Si, Ca, and Fe) strongly correlated with ash content, along with two trace elements (Mn and Ni) inherently present in the coal samples, as evaluation indicators.

The recoveries for Al, Si, Ca, Mn, Fe, and Ni are shown in Fig. 3. For samples with a particle size of I, the Si content is overestimated regardless of the dispersants used. This may be attributed to the contribution of quartz carrier to the determination of Si elemental content. Obviously, the content of Al and Si was significantly underestimated when sample with a particle size of II was used, which is caused by matrix effects resulting from large particle samples. However, the analytical results of Ca, Mn, Fe, and Ni were not significantly affected, a phenomenon that correlates with the positive relationship between their excitation cross-sections and atomic numbers (Z). With nearly constant excitation energy, these elements are more likely to be excited by X-rays compared to Al and Si, which have fewer electron shells. This difference may lead to less sensitivity to variations in sample particle size. For dispersant, ethylene glycol demonstrated better stability for sample with particle size II compared to 1 % Triton X-100, owing to its inherent viscosity. This advantage manifested in the determination of Ca and Fe. It is noteworthy that Ni exhibited relatively poor repeatability under all four analytical conditions, with relative RSDs exceeding 10 %. This could be attributed to the low Ni content in the sample (down to 8 mg kg^{-1}), as well as quantification errors arising from sampling variability, film formation quality, and background noise (Fig. 2 inset).

The DLs for Al, Si, Ca, Mn, Fe, and Ni are shown in Fig. 4, and are calculated using the following formula:

$$C_{DL} = 3C_i\sqrt{N_{BG}}\Big/N_i \quad (2)$$

where C_i and N_i are the content and net intensity of target element, respectively. N_{BG} is the background under the peak of target element.

With the reduction in sample particle size, the DLs of Ca, Mn, Fe, and Ni hardly showed significant enhancement. In contrast, the DLs for Al and Si were significantly improved, which could be attributed to the diminished absorption of fluorescence signals from light elements by the large particle samples. Specifically, for samples with particle size I, ethylene glycol as a dispersant slightly outperforms 1 % Triton X-100 in terms of achieving detection limits for target elements. Additionally, integrating the analysis results from Fig. 3, the YG_1 sample with particle size I prepared using ethylene glycol demonstrated better reproducibility, and the TXRF results aligned more closely with the reference values. Therefore, the optimal preparation strategy for coal samples is to mix the ethylene glycol with samples that have a particle size of I.

3.2. Validation of the TXRF method

To validate the accuracy and applicability of the TXRF analysis method, two CRMs were analyzed: ZBM1101 and ZBM1212. Fig. 5 illustrates the recoveries of Al, Si, Ca, Mn, and Fe. Although the recoveries for Al and Si fell within the ideal range of 95–105 %, their analytical results displayed relatively high fluctuations due to air absorption. The

RSD of 9.59 % and 10.98 % for Al in ZBM1101 and ZBM1212, respectively, while they were 7.99 % and 12.54 % for Si. Similar observations were reported in studies by Rodella [27] and Sharanov [28]. Furthermore, the analysis results for Si seemed unaffected by the quartz reflector, possibly because the high Si content in the two high-ash coal samples overshadowed the Si signal from the reflector, which could be considered inconsequential background noise. The comparison with the reference values of CRMs demonstrates good consistency of the TXRF analysis results, further validating the accuracy and applicability of this method.

3.3. Construction of coal ash prediction model

Following the research conducted in Sections 3.1 and 3.2, the TXRF analysis strategy for various types of coal samples was explored and validated. This strategy was applied to 19 coal samples, with three parallel measurements performed for each sample to ensure reliability. Subsequently, 14 of these coal samples were used as a training set to establish the PLS model, while the remaining 5 samples served as a test set to evaluate the model's performance.

Currently, in the reported applications of combined XRF/TXRF and machine learning algorithms for sample clustering or target value regression [9,10,25,29,30], the commonly used model predictor

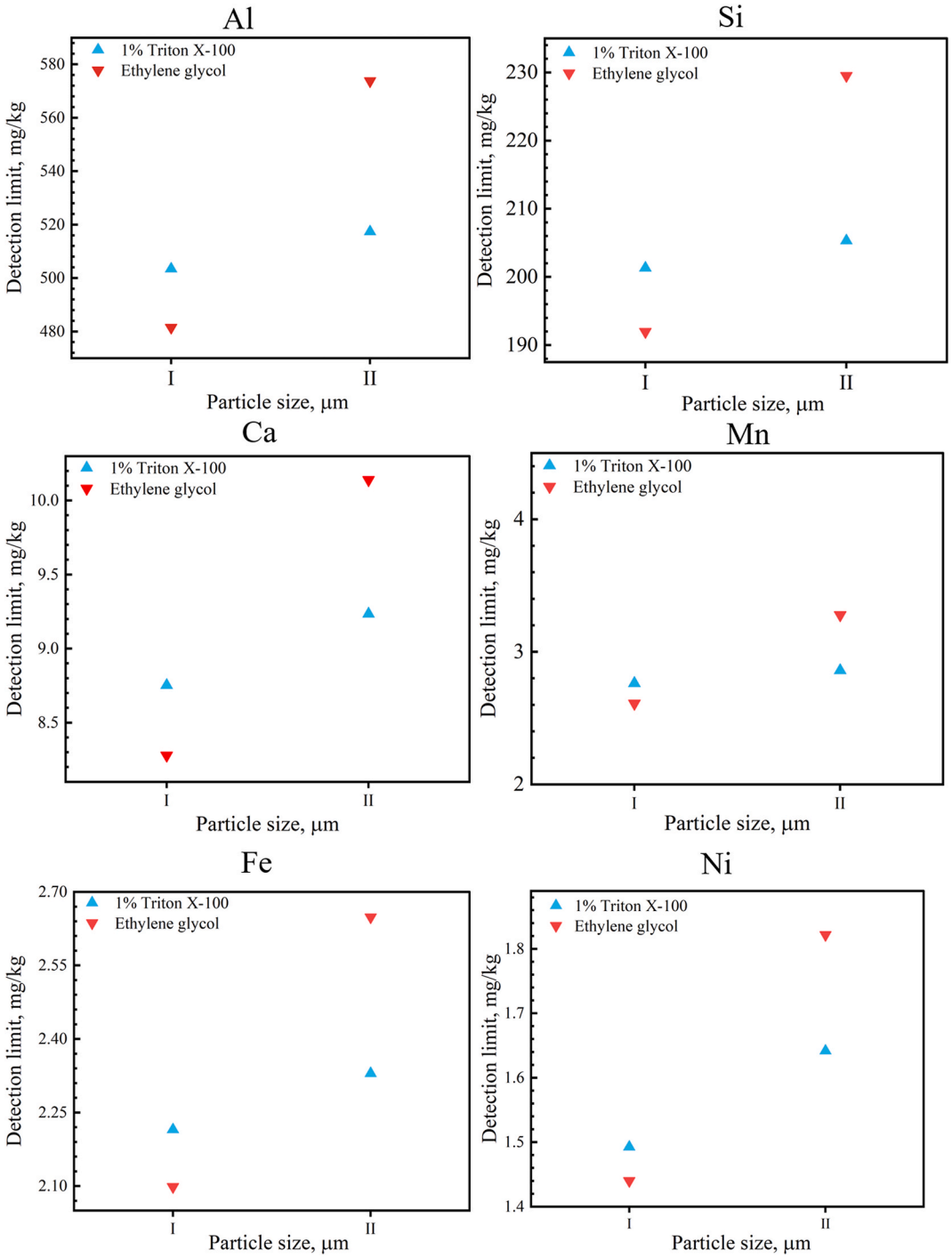

Fig. 4. The influence of sample particle size and dispersant type on the detection limit of Al, Si, Ca, Mn, Fe, and Ni.

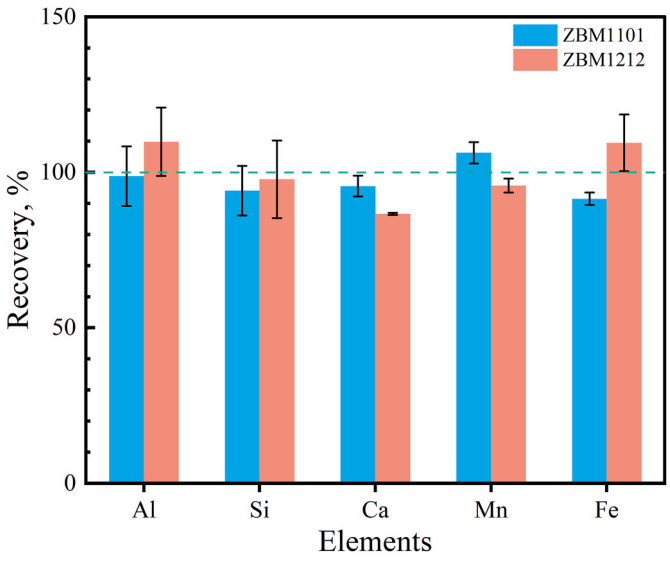

Fig. 5. Comparison of TXRF analysis results for ZBM1101 and ZBM1212 with standard values (error bars represent by the relative standard deviation of three tests).

variables are either the full spectral information or the elemental concentrations of the samples. To investigate the optimal predictor variables for establishing a PLS model based on TXRF, three different modeling approaches were considered: (1) normalizing the TXRF full spectrum of the coal samples using the net intensity of the IS; (2) normalizing the net intensities of the characteristic peaks for the 12 major and minor elements (Al, Si, K, Ca, Ti, Fe, Cr, Mn, Cu, Zn, Ni, and Sr) in the coal samples using the net intensity of the IS ; (3) directly using the concentrations of the aforementioned 12 elements in the coal samples. The purpose of normalizing the intensities relative to the IS is to correct potential errors arising from sample preparation and measurement, including variations in particle size, film thickness, among others. This method enhances the stability and reliability of the model. Fig. 6 presents the PLS models developed using these three different input variables.

As can be seen in Fig. 6, although both model B and model C

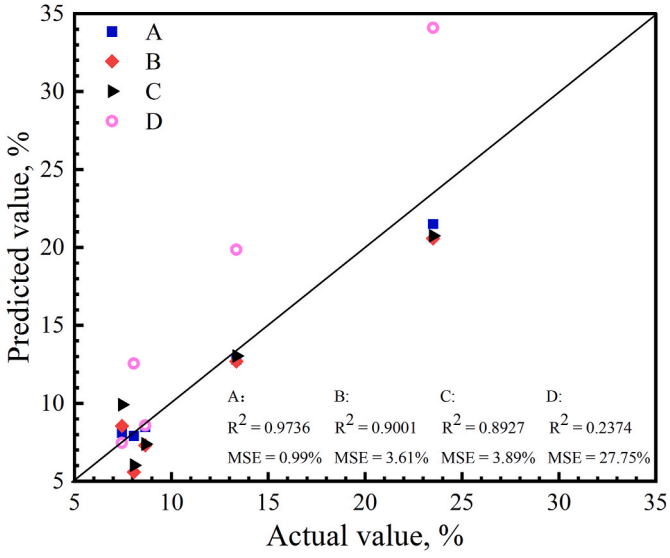

Fig. 6. The effect of three different types of input variables on the performance of the PLS model: (A) TXRF full spectrum normalized to the net intensity of Ga; (B) Net intensity of Al, Si, K, Ca, Ti, Fe, Cr, Mn, Cu, Zn, Ni and Sr normalized to Ga net intensity; (C) Contents of above 12 elements; (D) XRF full spectrum.

incorporate information on Al, Si, K, Ca, Ti, Fe, Cr, Mn, Cu, Zn, Ni, and Sr, the predictive accuracy of model C is slightly lower than that of B. This may be attributed to the large differences in the absolute concentrations of the elements, causing certain elemental intensities having a disproportionate magnified or minimized effect on the predictions of the model. In contrast, model B employed normalization using the IS net intensity, effectively minimizes the relative differences between variables and standardizes the elemental intensity values to a uniform magnitude. This approach eliminated the adverse impact of variations in absolute elemental concentrations on model construction. Nevertheless, the predictive performance of model B is still inferior to model A. This fact can be explained that model A utilized the full spectrum of coal samples normalized by the net intensity of IS, which not only ignores the interference of external factors, but also provides more comprehensive information about the samples, thus exhibiting superior predictive performance.

To assess the predictive performance of model A, its prediction results were compared with the model D (Fig. 6), which was constructed based on XRF full-spectrum. It is noteworthy that the XRF spectrum processing was based on the method proposed by Ref. [10]. Table 2 displays the predictions of the model A and D for five coal samples, with prediction accuracy assessed using the relative error (RE) between the predicted and actual values. The RE of model A was less than 10 %, with an average error of 5.01 %, demonstrating excellent predictive performance. In contrast, model D presented poorer stability, with an overall average error of 30.10 %, although achieving high accuracy for individual coal samples. This instability was particularly evident in predictions for coal samples with ash values of 8.06 %, 13.35 %, and 23.50 %, where relative errors ranged between 45.06 and 55.83 %. As illustrated in Fig. 2, both techniques can effectively obtain comprehensive compositional information from the samples, despite variations in the fluorescence signal intensities for the same element due to their different detection mechanisms. We hypothesize that the discrepancies may origin from the inherent physicochemical diversity among different coal types. TXRF primarily excites the surface layer of samples, thus effectively avoiding the effect of the physicochemical properties and matrix effects on the spectral information. This leads to an almost linear relationship between the concentrations of elements and their corresponding line intensities. Furthermore, the utilization of IS to normalize the TXRF full spectrum is also a pivotal factor contributing to the excellent analytical performance of the model. In contrast, XRF analysis is more susceptible to matrix effects and background scatter peaks due to analyzing samples at greater depths. This presents a considerable challenge in explaining the intrinsic relationship between spectral information and ash content, particularly when the available sample set is limited. Hence, XRF prediction models typically require an extensive set of training samples [23]. The deliberate selection of only 19 samples in this study highlights the superior performance of TXRF in situations involving multiple coal types, where it remains unaffected by matrix effects. With an increase in the numberof training samples, the predictive performance of TXRF is expected to improve further.

4. Conclusion

In this work, a novel method for ash content detection of various

Table 2
Actual values, predicted values, and relative errors between actual and predicted values for five samples.

Actual values	Model A	RE (%)	Model D	RE (%)
7.45	8.09	8.59	7.454	0.05
8.06	7.91	1.86	12.56	55.83
8.65	8.49	1.85	8.58	0.81
13.35	12.79	4.19	19.86	48.76
23.50	21.49	8.55	34.09	45.06

coals by combination TXRF with PLS was proposed. The suspension preparation method was selected for sample preparation, mixing 10 mg of sample powder with a particle size of less than 25 μm and 1 mL of ethylene glycol dispersant to prepare the suspension. The results of the TXRF analysis were compared with those obtained from ICP-MS and further validated through the analysis of ZBM1101 and ZBM1212. The recoveries of Al, Si, Ca, Mn, and Fe were within the range of 90–110 %, demonstrating the good accuracy and applicability of the TXRF method. Subsequently, this strategy was applied to the analysis of 19 coal samples. It was found that models constructed using these three predictive variables outperformed those based on XRF in terms of prediction performance. Especially in the model achieved the best performance using TXRF full spectrum normalized with the net intensity of the IS as predictive variables, achieving R^2 of 0.9736 and MSE of 0.99 %. The average prediction error was only 5.01 %, significantly lower than the 30.10 % observed with XRF under the same conditions. The study demonstrates that the proposed method combining TXRF with PLS for the rapid determination of coal ash content can effectively overcome the impact of complex coal sample physicochemical properties and matrix effects on analysis results. It also addresses the challenge of XRF requiring numerous standard samples for modeling in complex coal varieties, offering a new feasible path for accurate analysis of various coal types. The subsequent step will expand the scale of the dataset to further validate the effectiveness and applicability of this method.

CRediT authorship contribution statement

Yongsheng Zhang: Writing – review & editing, Writing – original draft, Validation, Software, Methodology, Investigation, Data curation, Conceptualization. **Jian Yuan:** Resources, Methodology, Conceptualization. **Rui Gao:** Software, Resources. **Yang Zhao:** Resources, Funding acquisition. **Zefu Ye:** Resources. **Zhujun Zhu:** Resources. **Peihua Zhang:** Resources. **Lei Zhang:** Writing – review & editing, Supervision, Project administration, Methodology, Funding acquisition, Conceptualization. **Wangbao Yin:** Supervision, Methodology, Funding acquisition, Conceptualization. **Suotang Jia:** Funding acquisition.

Declaration of competing interest

The authors declare that they have no known competing financial interests or personal relationships that could have appeared to influence the work reported in this paper.

Data availability

Data will be made available on request.

Acknowledgements

National Energy R&D Center of Petroleum Refining Technology (RIPP, SINOPEC); National Natural Science Foundation of China (NSFC) (12374377, 61975103 and 627010407); Changjiang Scholars and Innovative Research Team in University of Ministry of Education of China (IRT_17R70); 111 Project (D18001); Fund for Shanxi "1331KSC"; Supported by Fundamental Research Program of Shanxi Province (202103021223210).

References

[1] F.E. Huggins, Overview of analytical methods for inorganic constituents in coal, Int. J. Coal Geol. 50 (2002) 169–214, https://doi.org/10.1016/S0166-5162(02)00118-0.
[2] C.R. Ward, J.C. Taylor, Quantitative mineralogical analysis of coals from the callide basin, Queensland, Australia using X-ray Diffractometry and Normative interpretation, Int. J. Coal Geol. 30 (1996) 211–229, https://doi.org/10.1016/0166-5162(95)00044-5.
[3] K.H. Zhang, W.D. Wang, Z.Q. Lv, L.Z. Jin, D.H. Liu, M.C. Wang, Y.H. Lv, A CNN-based regression framework for estimating coal ash content on microscopic images, Meas. 189 (2022) 110589, https://doi.org/10.1016/j.measurement.2021.110589.
[4] R.K. Ileri, S. Haciyakupoglu, A.N. Esen, E. Oruçiglu, S. Erentürk, Assessment of environmental risk from coal using neutron activation analysis, Acta Phys. Pol., A 127 (2015) 1010–1012, https://doi.org/10.12693/APhysPolA.127.1010.
[5] W. Lyon, J. Emery, Neutron activation analysis applied to the study of elements entering and leaving a coal-fired steam plant, Int. J. Environ. Anal. Chem. 4 (1975) 125–133, https://doi.org/10.1080/03067317508071108.
[6] Y. Bai, J.X. Li, W.F. Zhang, L. Zhang, J.J. Hou, Y. Zhao, F. Chen, S.Q. Wang, G. Wang, X.F. Ma, et al., Accuracy enhancement of LIBS-XRF coal quality analysis through spectral intensity correction and piecewise modeling, Front. Physiol. 9 (2022) 823298, https://doi.org/10.3389/fphy.2021.823298.
[7] A. Haider, M.A. Rony, K.M. Abedin, Determination of the ash content of coal without ashing: a simple technique using laser-induced breakdown spectroscopy, Energy Fuels 27 (2013) 3725–3729, https://doi.org/10.1021/ef400566u.
[8] S. Legnaioli, B. Campanella, S. Pagnotta, F. Poggialini, V. Palleschi, Determination of ash content of coal by laser-induced breakdown spectroscopy, Spectrochim. Acta, Part B 155 (2019) 123–126, https://doi.org/10.1016/j.sab.2019.03.012.
[9] Z.P. Wen, H.T. Liu, M.Q. Zhou, C. Liu, C.C. Zhou, Explainable machine learning rapid approach to evaluate coal ash content based on X-ray fluorescence, Fuel 332 (2023) 125991, https://doi.org/10.1016/j.fuel.2022.125991.
[10] J.X. Li, R. Gao, Y. Zhang, S.Q. Wang, L. Zhang, W.B. Yin, S.T. Jia, Coal calorific value detection technology based on NIRS-XRF fusion spectroscopy, Chemosensors 11 (2023) 363, https://doi.org/10.3390/chemosensors11070363.
[11] G.V. Pashkova, A.A. Nikonova, S.D. Dylgerova, E.V. Chuparina, A.S. Maltsev, A. N. Zhilicheva, O.Y. Belozerova, L.P. Paradina, O.Y. Glyzina, I.V. Khanaev, Applicability of total reflection X-ray fluorescence for heavy metal analysis in lake baikal Sponges, X Ray Spectrom. (2023), https://doi.org/10.1002/xrs.3396.
[12] T.Y. Cherkashina, S.V. Panteeva, G.V. Pashkova, Applicability of direct total reflection X-ray fluorescence spectrometry for multielement analysis of geological and environmental objects, Spectrochim. Acta, Part B 99 (2014) 59–66, https://doi.org/10.1016/j.sab.2014.05.013.
[13] I. De La Calle, N. Cabaleiro, V. Romero, I. Lavilla, C. Bendicho, Sample pretreatment strategies for total reflection X-ray fluorescence analysis: a tutorial review, Spectrochim. Acta, Part B 90 (2013) 23–54, https://doi.org/10.1016/j.sab.2013.10.001.
[14] R. Fernández-Ruiz, TXRF spectrometry in the bioanalytical sciences: a brief review, X Ray Spectrom. 51 (2022) 279–293, https://doi.org/10.1002/xrs.3243.
[15] Y.S. Zhang, Y.X. He, W.Q. Zhou, G.Q. Mo, H. Chen, T. Xu, Review on the elemental analysis of polymetallic deposits by total-reflection X-ray fluorescence spectrometry, Appl. Spectrosc. Rev. 58 (2023) 428–441, https://doi.org/10.1080/05704928.2022.2130350.
[16] N. Szoboszlai, Z. Polgári, V.G. Mihucz, G. Záray, Recent trends in total reflection X-ray fluorescence spectrometry for biological applications, Anal. Chim. Acta 633 (2009) 1–18, https://doi.org/10.1016/j.aca.2008.11.009.
[17] Y.S. Zhang, Y.X. He, H. Chen, S.L. Wei, G.Q. Mo, T. Xu, J. Yuan, Exploratory studies on total reflection X-ray fluorescence spectrometry combined with slurry sampling for the multi-element analysis of Copper-Nickel Sulfide Ore, J. Anal. At. Spectrom. 38 (2023) 2648–2655, https://doi.org/10.1039/d3ja00287j.
[18] M. Regadío, S. Riaño, K. Binnemans, T. Vander Hoogerstraete, Direct analysis of metal Ions in solutions with high salt concentrations by total reflection X-ray fluorescence, Anal. Chem. 89 (2017) 4595–4603, https://doi.org/10.1021/acs.analchem.7b00097.
[19] R. Fernández-Ruiz, E.J. Friedrich, M.J. Redrejo, Effect of modulation of the particle size distributions in the direct solid analysis by total-reflection X-ray fluorescence, Spectrochim. Acta, Part B 140 (2018) 76–83, https://doi.org/10.1016/j.sab.2017.12.007.
[20] A.S. Maltsev, A.V. Ivanov, V.M. Chubarov, G.V. Pashkova, S.V. Panteeva, L. Z. Reznitskii, Development and validation of a method for multielement analysis of apatite by total-reflection X-ray fluorescence spectrometry, Talanta 214 (2020) 120870, https://doi.org/10.1016/j.talanta.2020.120870.
[21] F. Low, L. Zhang, Microwave digestion for the quantification of inorganic elements in coal and coal ash using ICP-OES, Talanta 101 (2012) 346–352, https://doi.org/10.1016/j.talanta.2012.09.037.
[22] X. Tian, L. Zhao, Determination of concentrations of Sr and Ba in coal and coal combustion by-Products: a comparison between results by ICP-MS and XRF techniques, Talanta 266 (2024) 124919, https://doi.org/10.1016/j.talanta.2023.124919.
[23] R. Gao, S.Q. Wang, J.X. Li, Z.H. Tian, Y. Zhang, L. Zhang, Z.F. Ye, Z.J. Zhu, W. B. Yin, S.T. Jia, Development and application of a rapid coal Calorific value analyzer based on NIRS-XRF, J. Anal. At. Spectrom. 38 (2023) 2046–2058, https://doi.org/10.1039/d3ja00197k.
[24] Z. Tian, J. Li, S. Wang, Y. Bai, Y. Zhao, L. Zhang, P. Zhang, Z. Ye, Z. Zhu, W. Yin, et al., Development and industrial application of LIBS-XRF coal quality analyzer by combining PCA and PLS regression methods, J. Anal. At. Spectrom. 38 (2023) 1421–1430, https://doi.org/10.1039/d3ja00015j.
[25] R. Guo, L. Zhang, Y.H. Zheng, H. Yao, Accurate and stable measurement of ash in coal by X-ray fluorescence spectrometry based on partial least squares, Front. Physiol. 10 (2022) 1054796, https://doi.org/10.3389/fphy.2022.1054796.
[26] G. Mateos-Aparicio, Partial least squares (PLS) methods: Origins, evolution, and application to social sciences, Commun. Stat. Theor. Methods 40 (2011) 2305–2317, https://doi.org/10.1080/03610921003778225.
[27] N. Rodella, A. Bosio, A. Zacco, L. Borgese, M. Pasquali, R. Dalipi, L.E. Depero, V. Patel, P.A. Bingham, E. Bontempi, Arsenic stabilization in coal fly ash through

the employment of waste materials, J. Environ. Chem. Eng. 2 (2014) 1352–1357, https://doi.org/10.1016/j.jece.2014.05.011.
[28] P.Y. Sharanov, N.V. Alov, Total reflection X-ray fluorescence analysis of solid metallurgical samples, J. Anal. Chem. 73 (2018) 1085–1092, https://doi.org/10.1134/s1061934818110126.
[29] X.L. Zhang, W.B. Jia, X.R. Tang, Q. Shan, Q.Y. Chen, C. Cheng, J.F. Shao, Y.S. Ling, D.Q. Hei, Geographical discrimination of Pu-Erh Tea by the determination of elements by low-power total reflection X-ray fluorescence (TXRF) and Caffeine and Polyphenols by spectrophotometry, Anal. Lett. 56 (2023) 556–575, https://doi.org/10.1080/00032719.2022.2093891.
[30] A.S. Maltsev, N.N. Umarova, G.V. Pashkova, M.M. Mukhamedova, D.L. Shergin, V. V. Panchuk, D.O. Kirsanov, E.I. Demonterova, Combination of total-reflection X-ray fluorescence method and chemometric techniques for provenance study of archaeological ceramics, Mol 28 (2023) 1099, https://doi.org/10.3390/molecules28031099.